Steric Control of Electron Transfer. Changeover from Outer-Sphere to Inner-Sphere Mechanisms in Arene/Quinone Redox Pairs

Stephan M. Hubig, Rajendra Rathore, and Jay K. Kochi*

Contribution from the Department of Chemistry, University of Houston, Houston, Texas 77204-5641

Received August 28, 1998

Abstract: The various aromatic hydrocarbons (Chart 2) constitute a sharply graded series of sterically encumbered (unhindered, partially hindered, and heavily hindered) donors in electron transfer (ET) to quinones (Chart 1). As such, steric effects provide the quantitative basis to modulate (and differentiate) outer-sphere and inner-sphere pathways provided by matched pairs of hindered and unhindered donors with otherwise identical electron-transfer properties. Thus the **hindered donors** are characterized by (a) bimolecular rate constants (k_2) that are temperature dependent and well correlated by Marcus theory, (b) no evidence for the formation of (discrete) encounter complexes, (c) high dependency on solvent polarity, and (d) enhanced sensitivity to kinetic salt effects—all diagnostic of outer-sphere electron-transfer mechanisms. Contrastingly, the analogous **unhindered donors** are characterized by (a) temperature-independent rate constants (k_2) that are 10^2 times faster and rather poorly correlated by Marcus theory, (b) weak dependency on solvent polarity, and (c) low sensitivity to kinetic salt effects—all symptomatic of inner-sphere ET mechanisms arising from the preequilibrium formation of encounter complexes with charge-transfer (inner-sphere) character. Steric encumbrances which inhibit strong electronic (charge-transfer) coupling between the benzenoid and quinonoid π systems are critical for the mechanistic changeover. Thus, the classical outer-sphere/inner-sphere distinction (historically based on coordination complexes) is retained in a modified form to provide a common terminology for inorganic as well as organic (and biochemical) redox systems.

Introduction

In bimolecular electron transfer (ET) between freely diffusing donors and acceptors in solution, the nuclear prearrangement of the reactants in the transition state—with its critical donor/acceptor distance and orbital overlap—limits the intrinsic rate of the electron exchange.[1,2] As a result, all theoretical calculations of ET rate constants invoke far-reaching assumptions on the relative orientation and electronic interaction of the donor and the acceptor in the transition state.[3]

Owing to the intrinsic lifetime of transition states, their direct (spectroscopic) observation constitutes an experimental challenge.[4] However, attempts have been made to predict structures and degrees of donor/acceptor bonding in various ET transition states by different theoretical methods.[5] Electronic coupling that promotes electron transfer between redox partners is revealed experimentally by charge-transfer (CT) interactions extant in the donor/acceptor precursor or encounter complex prior to electron transfer, and the degree of charge transfer as defined by Mulliken theory can be taken as a measure of the donor/acceptor bonding.[6−8] For example, we recently showed[9] that electron transfer from arene donors to photoactivated quinones occurs via encounter complexes (EC) with substantial charge-transfer bonding, by the observation of the near-IR absorption bands and relatively high formation constants (K_{EC}). Furthermore, the resulting two-step quenching mechanism involving encounter-complex formation (K_{EC}) followed by electron transfer (k_{ET}) leads to second-order rate constants (k_2) that are composites of K_{EC} and k_{ET}.[10,11] In this study, we show how sterically encumbered electron donors can circumvent the kinetics complications arising from the formation of encounter complexes. The systematic comparison of the electron-transfer kinetics of hindered versus unhindered electron donors will probe the effects of steric hindrance on the ET transition state. [12,13]

(1) Eyring, H.; Polanyi, M. *Z. Phys. Chem.* **1931,** *B12*, 279. (b) Glasstone, S.; Laidler, K. J.; Eyring, H. *The Theory of Rate Processes*; McGraw-Hill: New York, 1941.

(2) Ultrafast rate constants of $k_{ET} > 2 \times 10^{12}$ s^{-1} have been determined for electron-transfer processes within electron donor/acceptor complexes. See: (a) Wynne, K.; Galli, C.; Hochstrasser, R. M. *J. Chem. Phys.* **1994**, *100*, 4797. (b) Asahi, T.; Mataga, N. *J. Phys. Chem.* **1989**, *93*, 6575. See also: Hannappel, T.; Burfeindt, B.; Storck, W.; Willig, F. *J. Phys. Chem.* **1997**, *B101*, 6799.

(3) Traditionally, electron-transfer reactions are classified as either "inner-sphere" (bonded) or "outer-sphere" (nonbonded) processes. See: (a) Taube, H. *Electron-Transfer Reactions of Complex Ions in Solution*; Academic Press: New York, 1970. (b) Cannon, R. D. *Electron-Transfer Reactions*; Butterworth: London, 1980. (c) Zipse, H. *Angew. Chem., Int. Ed. Engl.* **1997**, *36*, 1697. (d) Eberson, L. *New J. Chem.* **1992**, *16*, 151. (e) Tributsch, H.; Pohlmann, L. *Science* **1998**, *279*, 1891.

(4) See: (a) Polanyi, J. C.; Zewail, A. H. *Acc. Chem. Res.* **1995**, *28*, 119. (b) Zhong, D.; Zewail, A. H. *J. Phys. Chem.* **1998**, *A102*, 4031.

(5) Sastry, G. N.; Shaik, S. *J. Am. Chem. Soc.* **1998**, *120*, 2131. (b) Eberson, L.; Shaik, S. S. *J. Am. Chem. Soc.* **1990**, *112*, 4484. (c) Bertran, J.; Gallardo, I.; Moreno, M.; Savéant, J.-M. *J. Am. Chem. Soc.* **1996**, *118*, 5737. (d) Su, J. T.; Zewail, A. H. *J. Phys. Chem.* **1998**, *A102*, 4082.

(6) Mulliken theory[7] describes the wave function (Ψ_{AD}) of a charge-transfer complex as principally the sum of the dative (bonding) function (ψ_1) and the "no-bond" function (ψ_0), *i.e.* $\Psi_{AD} = \mathbf{a}\psi_0$ (A, D) + $\mathbf{b}\psi_1$ (A$^-$, D$^+$) + ...

(7) Mulliken, R. S. *J. Am. Chem. Soc.* **1950**, *72*, 600. (b) Mulliken, R. S. *J. Am. Chem. Soc.* **1952**, *74*, 811. (c) Mulliken, R. S.; Person, W. M. *Molecular Complexes*; Wiley: New York, 1969.

(8) On the basis of Mulliken theory,[7] the degree of charge transfer is defined as the ratio $(\mathbf{b}/\mathbf{a})^2$ of the mixing coefficients **a** and **b** of the no-bond and the dative wave functions, respectively. For the experimental determination of $(\mathbf{b}/\mathbf{a})^2$, see: (a) Ketelaar, J. A. A. *J. Phys. Radium* **1954**, *15*, 197. (b) Tamres, M.; Brandon, M. *J. Am. Chem. Soc.* **1960**, *82*, 2134. See also: (c) Briegleb, G. *Elektronen-Donator-Acceptor-Komplexe*; Springer: Berlin, 1961.

(9) Rathore, R.; Hubig, S. M.; Kochi, J. K. *J. Am. Chem. Soc.* **1997**, *119*, 11468.

(10) Hubig, S. M.; Kochi, J. K. *J. Am. Chem. Soc.* In press.

(11) Compare: Rehm, D.; Weller, A. *Isr. J. Chem.* **1970**, *8*, 259.

10.1021/ja9831002 CCC: $18.00
Published on Web 01/13/1999

Chart 1. Quinone Acceptors

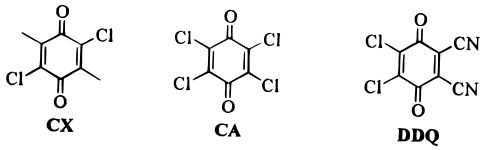

	CX	CA	DDQ	
E^*_{red}	1.62	2.15	2.71	[V *vs.* SCE]

We employ benzoquinones in their photoactivated state as electron acceptors and monitor electron transfer from various hindered and unhindered arene donors by time-resolved laser-flash experiments. Chloranil (**CA**), 2,5-dichloroxyloquinone (**CX**), and 2,3-dichloro-5,6-dicyano-1,4-benzoquinone (**DDQ**) in Chart 1 are electron acceptors of choice since their long-lived (μs) excited (triplet) states exhibit high reduction potentials ($E^*_{red} > 1.6$ V vs SCE).[14] The series of methyl-substituted benzenes and their sterically encumbered analogues in Chart 2 are selected on the basis of similar one-electron oxidation potentials.[15]

The electron acceptors and donors in Charts 1 and 2 are especially well-suited for delineating the effects of steric encumbrance on the mechanism of electron transfer since (a) the driving force can be tuned over a wide range without essential changes in the size and orientation of the redox centers and (b) steric hindrance can be introduced by bulky substituents without affecting the driving force.[16] Thus, we will demonstrate that increases in the donor−acceptor distance caused by steric hindrance induce a changeover in the electron-transfer mechanism owing to the substantial diminution of the donor/acceptor orbital overlap.[17] Unhindered donors form distinct encounter complexes with the quinone acceptors—the charge-transfer absorptions of which reveal substantial electronic coupling of the donor/acceptor orbitals comparable to that found in mixed-valence metal complexes.[26] Since the latter are used as prototypical models for the bridged-activated complex in inner-sphere electron transfers,[23,27] we adopt the term "inner-sphere" to also describe the electron transfer between donors and acceptors in the encounter complex that are not covalently bonded but are nonetheless strongly coupled.[28−30] The critical experimental evidence for inner-sphere character is the pronounced sensitivity of the electron-transfer rates to steric hindrance and the weakening of the electronic coupling between the donor and

(12) Rathore, R.; Lindeman, S. V.; Kochi, J. K. *J. Am. Chem. Soc.* **1997**, *119*, 9393. (b) For the effects of steric hindrance on exciplex formation, see: Jacques, P.; Allonas, X.; Suppan, P.; Von Raumer, M. *J. Photochem. Photobiol.* **1996**, *A 101*, 183.

(13) The precursor or encounter complex (prior to electron transfer) and the ET transition state are assumed to be structurally similar and exhibit more or less comparable donor/acceptor interactions. See: (a) Sutin, N. *Acc. Chem. Res.* **1968**, *1*, 225. Compare also: (b) Marcus, R. A. *J. Chem. Phys.* **1956**, *24*, 966. (c) Marcus, R. A. *Angew. Chem., Int. Ed. Engl.* **1993**, *32*, 1111 and references therein.

(14) The reduction potential of the photoactivated quinones (E^*_{red}) is taken as the sum of the quinone triplet energy ($E_T \cong 2.2$ eV) and the reduction potential of the quinone in its ground state. For the triplet energies (E_T) of the quinones, see: (a) Shcheglova, N. A.; Shigorin, D. N.; Yakobson, G. G. Y.; Tushishvili, L. Sh. *Russ. Phys. Chem.* **1969**, *43*, 1112. (b) Trommsdorff, H. P.; Sahy, P.; Kahane-Paillous *Spectrochim. Acta* **1968**, *24A*, 785. (c) Herre, W.; Weis, P. *Spectrochim. Acta* **1973**, *29A*, 203. (d) Koboyama, A. *Bull. Chem. Soc. Jpn.* **1962**, *35*, 295. For the reduction potentials of the quinones (in the ground state), see: (e) Mann, C. K.; Barnes, K. K. *Electrochemical Reactions in Non-Aqueous Systems*; Dekker: New York, 1970. (f) Peover, J. E. *J. Chem. Soc.* **1962**, 4540.

(15) (a) Howell, J. O.; Goncalvez, J. M.; Amatore, C.; Klasinc, L.; Wightman, R. M.; Kochi, J. K. *J. Am. Chem. Soc.* **1984**, *106*, 3968. (b) Note that the steric encumbrance of hindered donors such as hexaethylbenzene (**HEB**) relative to hexamethylbenzene (**HMB**) is gauged by their increased van der Waals thickness of $2r \geq 6.4$ Å arising from the pendant methyl groups (illustrated below)

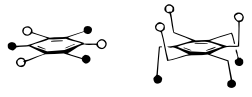

that discourage any close cofacial approach to the benzenoid (π-) chromophore (see Chart 3).[12] In addition, a few "partially" hindered donors are included in this study to demonstrate the effects of the (ring) position of bulky substituents on the overall steric encumbrance of the arene.

(16) Furthermore, the use of uncharged redox partners allows the electron transfer to be studied in aprotic polar as well as nonpolar solvents (to avoid the rather unique ionic solvation by water). Note also that the charge-delocalization and charge-transfer ability is optimized in such multiatom (expanded) redox centers of the donor/acceptor pair.

(17) Orbital overlap is commonly described by the electronic coupling matrix element V (or H_{AB}), which is assumed (within the limit of weak coupling) to exhibit an exponential falloff with the donor−acceptor distance R, i.e., $V = V_0 \exp\{-\beta (R - R_0)\}$ with R_0 being the donor−acceptor distance at van der Waals contact. (b) See: Endicott, J. F.; Kumar, K.; Ramasami, T.; Rotzinger, F. P. *Prog. Inorg. Chem.* **1983**, *30*, 141 and references therein. (c) Weak coupling ($V < 100$ cm^{-1} or 0.3 kcal mol^{-1}) of the donor and acceptor orbitals is found in solvent-separated ion-radical pairs[18] and in donor/acceptor couples separated by rigid spacers.[19] (d) Strong coupling is observed in contact ion-radical pairs ($V \cong 800-1000$ cm^{-1}),[18, 20] exciplexes ($V \cong 1300$ cm^{-1}),[21] cyclophane-derived charge-transfer complexes ($V \cong 1300-1800$ cm^{-1}),[22] and binuclear (mixed-valence) metal complexes[23, 24a] (*e.g.*, pyrazine-bridged:[24] $V \cong 300-700$ cm^{-1}; cyano-bridged:[25] $V \cong 1500-2100$ cm^{-1}).

(18) Gould, I. R.; Young, R. H.; Moody, R. E.; Farid, S. *J. Phys. Chem.* **1991**, *95*, 2068. (b) Gould, I. R.; Young, R. H.; Mueller, L. J.; Farid, S. *J. Am. Chem. Soc.* **1994**, *116*, 8176. (c) Tachiya, M.; Murata, S. *J. Am. Chem. Soc.* **1994**, *116*, 2434.

(19) Miller, J. R.; Calcaterra, L. T.; Closs, G. L. *J. Am. Chem. Soc.* **1984**, *106*, 3047. (b) Closs, G. L.; Calcaterra, L. T.; Green, N. J.; Penfield, K. W.; Miller, J. R. *J. Phys. Chem.* **1986**, *90*, 3673. (c) Wasilewski, M. R.; Niemczyk, M. P.; Svec, W. A.; Pewitt, E. B. *J. Am. Chem. Soc.* **1985**, *107*, 1080. (d) Paddon-Row, M. N. *Acc. Chem. Res.* **1994**, *27*, 18.

(20) Gould, I. R.; Noukakis, D.; Gomez-Jahn, L.; Goodman, J. L.; Farid, S. *J. Am. Chem. Soc.* **1993**, *115*, 4405.

(21) Gould, I. R.; Young, R. H.; Mueller, L. J.; Albrecht, A. C.; Farid, S. *J. Am. Chem. Soc.* **1994**, *116*, 8188.

(22) Benniston, A. C.; Harriman, A.; Philp, D.; Stoddart, J. F. *J. Am. Chem. Soc.* **1993**, *115*, 5298.

(23) Haim, A. *Prog. Inorg. Chem.* **1983**, *30*, 273.

(24) Creutz, C. *Prog. Inorg. Chem.* **1983**, *30*, 1. (b) Creutz, C.; Taube, H. *J. Am. Chem. Soc.* **1969**, *91*, 3988. (c) Goldsby, K. A.; Meyer, T. J. *Inorg. Chem.* **1984**, *23*, 3002.

(25) Burewicz, A.; Haim, A. *Inorg. Chem.* **1988**, *27*, 1611.

(26) Compare the electronic coupling matrix elements of organic donor/acceptor exciplexes[21] with those of mixed-valence metal complexes.[23−25]

(27) Astruc, D. *Electron Transfer and Radical Processes in Transition-Metal Chemistry*; VCH: New York, 1995; p 30.

(28) This view of "inner-sphere" electron transfer goes beyond its original definition[3a] that is largely based on ionic (inorganic) coordination complexes by including uncharged (organic) redox systems with measurable donor/acceptor coupling. We believe it is highly desirable to retain the classical inner-sphere/outer-sphere distinction in this modified form (to avoid inventing new terms) so that a universal and common terminology can be applied to describe electron-transfer mechanisms in all branches of inorganic chemistry, organic chemistry, and biochemistry.

(29) From the practical point of view, this distinction between inner-sphere and outer-sphere electron transfers based on the (experimentally observable) electronic coupling of donor and acceptor is rather straightforward. First, it circumvents the (quantitative) ambiguities inherent to chemically based differentiations such as ligand exchange, isotopic labeling, bridged intermediate, etc. in inner-sphere electron transfers.[23,27] Second, anomalies in the outer-sphere behavior (i.e., deviations from Marcus theory) need not to be explained by approximate corrections of the work terms, etc.,[3b] if they can be accounted for by electronic coupling terms in an inner-sphere model.[17b,41b]

(30) Note also that an inner-sphere/outer-sphere distinction based on orbital overlap allows for a continuum of intermediate cases to exist between the two idealized models that depend on the degree of electronic coupling. Moreover, the simultaneous occurrence of both mechanisms is readily accounted for in medium-strong interactions. See: (a) Taube, H.; Myers, H. *J. Am. Chem. Soc.* **1954**, *76*, 2103. (b) Melvin, W. S.; Haim, A. *Inorg. Chem.* **1977**, *16*, 2016. (c) Connocchioli, T. J.; Hamilton, E. J.; Sutin, N. *J. Am. Chem. Soc.* **1965**, *87*, 926. For the suggestion of a continuum, see: (d) Fukuzumi, S.; Wong, C. L.; Kochi, J. K. *J. Am. Chem. Soc.* **1980**, *102*, 2928. (e) Rosseinsky, D. R. *Chem. Rev.* **1972**, *72*, 215. (f) Eberson, L. *Adv. Phys. Org. Chem.* **1982**, *18*, 79.

Chart 2. Arene Donors

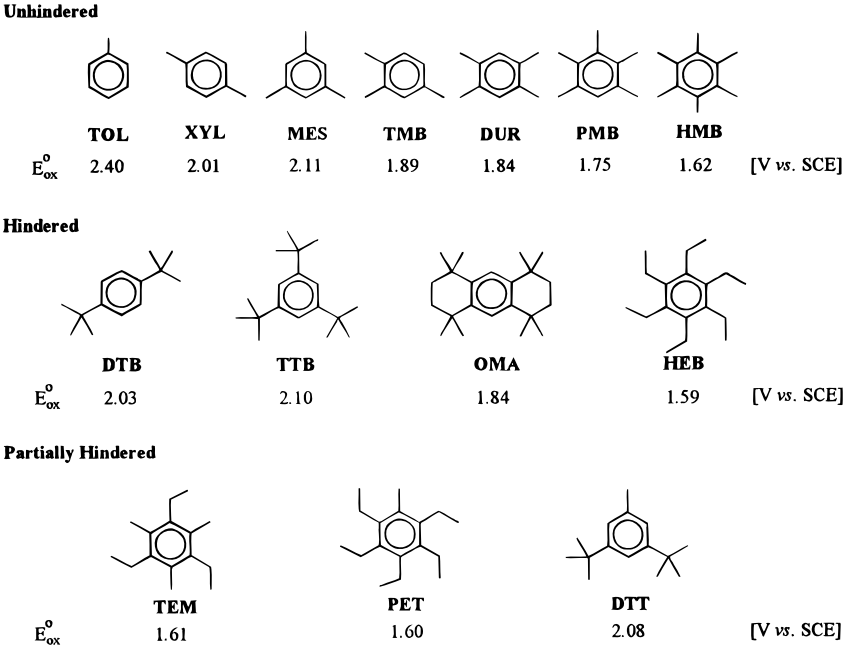

the acceptor due to an increased distance. Most importantly, a substantial increase in the donor−acceptor distance due to bulky substituents in hindered donors ultimately leads to outer-sphere electron transfer with no or very little sensitivity to steric hindrance.[31]

Results

I. Electron Transfer from Aromatic Donors to Photoactivated Quinones. A. Determination of the Second-Order Rate Constants (k_2). Photoexcitation of the quinones (**Q**) in Chart 1 with a 10-ns laser pulse at 355 nm spontaneously generates their excited triplet states (**Q***) with unit efficiency in acetonitrile solution, and the characteristic absorption spectrum of **Q*** decays to the spectral baseline on the microsecond time scale with $k_d < 5 \times 10^4$ s^{-1}.[9] However, **Q*** decays significantly faster in the presence of the aromatic donors (ArH), and the concomitant formation of the quinone anion radical ($\mathbf{Q}^{-\bullet}$) and the arene cation radical ($ArH^{+\bullet}$) is observed with identical (first-order) rate constants for **Q*** decay and ion-radical formation. Quantitative analysis of the time-resolved absorption spectra (see the Experimental Section) establishes the formation of the ion radicals $\mathbf{Q}^{-\bullet}$ and $ArH^{+\bullet}$ to occur in a 1:1 molar ratio with unit efficiency, i.e. $\Phi_{ion} \cong 1$,[32]

$$\mathbf{Q}^* + \mathrm{ArH} \xrightarrow[(CH_3CN)]{k_2} \mathbf{Q}^{-\bullet} + \mathrm{ArH}^{+\bullet} \qquad (1)$$

The kinetics of the bimolecular electron transfer in eq 1 is examined under pseudo-first-order conditions by monitoring the decay of **Q*** (or the simultaneous growth of $\mathbf{Q}^{-\bullet}$ and $ArH^{+\bullet}$) as a function of excess arene concentration ([ArH]). At low ArH concentrations of [ArH] < 0.01 M, the observed (first-order) rate constant (k_{obs}) increases linearly with the arene concentration, and the slope of the pseudo-first-order plot yields the second-order rate constant (k_2) listed in Table 1 for electron transfer from ArH to **Q*** in eq 1.

B. Steric Effects. The k_2 values for the various quinone/arene combinations in Table 1 are strongly affected by the steric encumbrance of the arene donor. Thus the rate constants for electron transfer from sterically hindered *tert*-butyl donors **TTB** and **DTB** as well as the tetra- and hexa-substituted analogues **OMA** and **HEB** are reduced by a factor of 100 (or more) compared to k_2 of the analogous unhindered donors **MES**, **XYL**, **DUR**, and **HMB**, respectively, as paired mates with essentially the same donor properties (compare E^0_{ox} values in Chart 2). Such a trend is independent of the quinone acceptor, as seen in Table 1 by the pairwise comparisons of the even/odd entries of k_2 at comparable driving forces ($-\Delta G_{ET}$).

Table 1. Electron-Transfer Rate Constants and Ion Yields

			k_2 [10^6 M^{-1} s^{-1}][c]		
	Q/ArH[a]	ΔG_{ET} [eV][b]	CH_3CN	CH_2Cl_2	Φ_{ion}[d]
1	**CX/MES**	+0.49	4.0 (3.9)	5.3 (8.4)	>0.3
2	**CX/TTB**	+0.39	0.4	*e*	*e*
3	**CX/XYL**	+0.44	2.4 (9.1)	3.5 (4.6)	>0.45
4	**CX/DTB**	+0.41	0.8	*e*	>0.54
5	**CX/TMB**	+0.27	40 (50)	15(18)	>0.85
6	**CA/TOL**	+0.25	10 (10)	15(18)	>0.72
7	**CX/DUR**	+0.21	2560 (2550)	300(380)	0.99
8	**CX/OMA**	+0.22	50	17	*e*
9	**CX/PMB**	+0.13	4000	1500 (2200)	*e*
10	**CX/HMB**	±0	5140	5500 (7300)	1.03
11	**CX/HEB**	−0.03	970	160	1.03
12	**CA/MES**	−0.04	4400	1150 (1080)	0.94
13	**CA/TTB**	−0.14	900	14	1.02
14	**CA/XYL**	−0.09	5400	1200 (800)	0.95
15	**CA/DTB**	−0.12	1300	3	1.15
16	**CA/DUR**	−0.32	6000	12000	0.95
17	**CA/OMA**	−0.31	2750	1900	*e*
18	**CA/HMB**	−0.53	8000	12000	0.98
19	**CA/HEB**	−0.56	6900	8000	1.14
20	**DDQ/HMB**	−1.02	21000	*e*	*e*
21	**DDQ/HEB**	−1.05	16000	*e*	*e*

[a] Quinone/arene combination (see Charts 1 and 2). [b] Electron-transfer driving force as determined from eq 2. [c] Second-order rate constant for the electron transfer from the arene donor to the photoactivated quinone. [d] Ion yield (±0.1) as determined by benzophenone actinometry (see the Experimental Section). [e] Not measured.

(31) Juillard, M.; Chanon, M. *Chem. Rev.* **1983**, *83*, 425.

(32) In some cases (entries 1−4 in Table 1), the ion-radical yields (Φ_{ion}) are less than unity, and k_2 in Table 1 represents the upper limit of the second-order rate constant for electron transfer.

Table 2. Solvent Dependence of the Electron-Transfer Rates

	k_2 [10^8 M^{-1} s^{-1}][b]			
Q/ArH[a]	CH_3CN ($\epsilon = 35.9$)[c]	CH_2Cl_2 ($\epsilon = 8.9$)[c]	$CHCl_3$ ($\epsilon = 4.8$)[c]	CCl_4 ($\epsilon = 2.2$)[c]
CX/HMB	51.4	55	23	23
CX/TEM	32	33	17	7.6
CX/PET	17	20	14	1.7
CX/HEB	9.7	1.6	0.4	0.04
CX/DUR	25.6	3.0	2.3	1.1
CX/OMA	<0.5	0.17	0.15	0.02
CA/MES	39	12	6.7	2.5
CA/DTT	24	8.8	5.3	0.86
CA/TTB	9	0.14	0.16	0.003
CA/XYL	54	12	6.6	1.8
CA/DTB	13	0.03	0.02	0.002

[a] Quinone/arene combination (see Charts 1 and 2). [b] Second-order rate constant for the electron transfer from the arene donor to photoactivated quinone. [c] Dielectric constant (see ref 33c).

C. Solvent Effect. Electron transfer from hindered donors to quinone is also strongly affected by solvent polarity, whereas the rate constants for electron transfer from the unhindered donors do not vary significantly from acetonitrile to dichloromethane.[33] The pronounced solvent effect on the rate constants (k_2) of the hindered donor/acceptor pairs becomes even more evident with the solvent variation presented in Table 2. Thus,the rate constants for electron transfer from the hindered donors **HEB**, **OMA**, **TTB**, and **DTB** progressively decrease (up to 4 orders of magnitude) from the polar solvent acetonitrile ($\epsilon =$ 35.9) to dichloromethane ($\epsilon = 8.9$), chloroform ($\epsilon = 4.8$), and the nonpolar solvent carbon tetrachloride ($\epsilon = 2.2$).[33] In strong contrast, the rate constants for the unhindered analogues hexamethylbenzene (**HMB**), durene (**DUR**), mesitylene (**MES**), and *p*-xylene (**XYL**) undergo minor change (at most by a factor of 25) as a result of the same solvent variation. The effects of partial hindrance on the electron-transfer kinetics are also shown in Table 2 by the falloff in k_2 in all solvents from the successive replacement of the methyl substituents of hexamethylbenzene by ethyl groups (see entries 1−4 in Table 2). It is noteworthy that the rate constants do not decrease monotonically with the number of ethyl substituents, but an abrupt drop in the rate constants occurs in the interval from pentaethyltoluene (**PET**) to hexaethylbenzene (**HEB**). Similarly, the difference in the rate constants between tri-*tert*-butylbenzene (**TTB**) and di-*tert*-butyltoluene (**DTT**) is much larger than that between **DTT** and mesitylene (**MES**, see entries 7−9). The solvent dependence of the rate constants follows the same pattern—the partially hindered arene donors showing a moderate solvent effect similar to that observed for the unhindered donors. On the other hand, substantial changes of the ET rate constants are solely observed for the hindered donors due to solvent polarity (vide supra).

D. Salt Effects. The effect of added salt on the rate constants for electron transfer from variously hindered donors to photoactivated quinones in chloroform is presented in Table 3. In contrast to the unhindered donors, which do not exhibit a significant kinetic salt effect,[9,33b] the electron-transfer kinetics from hindered donors is quite sensitive to the presence of inert salt. Thus the bimolecular rate constants (k_2) increase by up to a factor of 5 when 0.1 M tetra-*n*-butylammonium hexafluorophosphate is deliberately added to the solution of quinone and hindered donor in chloroform.

Table 3. Salt Effects on Electron-Transfer Rates

	k_2 [10^8 M^{-1} s^{-1}][c]	
Q/ArH[b]	no salt[a]	0.1 M salt[a]
CX/HEB	0.42	2.41
CA/TTB	0.16	0.38
CA/DTB	0.02	0.41

[a] Tetra-*n*-butylammonium hexafluorophosphate in $CHCl_3$. [b] Quinone/arene combination (see Charts 1 and 2). [c] Second-order rate constant for the electron transfer from the arene donor to photoactivated quinone.

II. Driving-Force ($-\Delta G_{ET}$) Dependence of the Electron-Transfer Rate Constant. The driving-force dependence of electron transfer from ArH to **Q***, as given by the free energy change (ΔG_{ET}), is based on eq 2,[11]

$$\Delta G_{ET} = E^0_{ox} - E^*_{red} + \text{constant} \qquad (2)$$

where E^0_{ox} is the oxidation potential of the benzene donor (ArH)[15] and E^*_{red} is the reduction potential of the photoactivated quinone (**Q***).[14] The second-order rate constants (k_2) in Table 1 vary over 4 orders of magnitude from the most endergonic electron-transfer couple (**CX***/**MES**) to the most exergonic couple (**DDQ***/**HMB**). Figure 1 shows that the rate constants (k_2) do not increase linearly with the driving force ($-\Delta G_{ET}$) of the electron transfer. A strong increase is observed over more than 3 orders of magnitude in the endergonic and slightly exergonic region (-0.5 eV $< \Delta G_{ET} <$ 0.5 eV), and this is followed by a limiting value of $k_2 \cong 10^{10}$ M^{-1} s^{-1} which remains unchanged over the exergonic region (-1.5 eV $< \Delta G_{ET} < -0.5$ eV). A closer scrutiny reveals that the hindered (filled circles) and the unhindered (open circles) donor/acceptor pairs show quite different driving-force dependences.

A. Hindered Donors. The ET rate constants of the hindered donors (Table 1 and solid circles in Figure 1) can readily be simulated by the Marcus free-energy correlation (dashed line),[13] *i.e.*

$$k_2 = k_{diff}/[1 + A \exp(\Delta G^{\ddagger}/RT)] \qquad (3)$$

$$A = k_{diff}/ZK \qquad (4)$$

$$\Delta G^{\ddagger} = (\lambda/4)[1 + (\Delta G_{ET} - \alpha)/\lambda)]^2 \qquad (5)$$

where k_2 is the second-order rate constant for the bimolecular electron transfer, k_{diff} is the rate constant for diffusion,[34] Z is the frequency factor, $K = k_{diff}/k_{-diff}$ is the equilibrium constant for diffusional encounters,[35] $\Delta G^{\ddagger}$ is the free activation enthalpy, ΔG_{ET} is the free energy as defined in eq 2, λ is the reorganization energy, and α is a shift parameter applied to triplet quenching.[36e] The close match between the experimental data (solid circles) and the Marcus correlation (dashed line) obtains in Figure 1 between -0.5 eV $< \Delta G_{ET} <$ 0.5 eV.[36]

(33) In dichloromethane solution and other less polar solvents, the quenching of **Q*** by polymethylbenzenes ($ArCH_3$) results in the formation of semiquinone (**QH**$^{\bullet}$) and benzyl ($ArCH_2^{\bullet}$) radicals. However, salt-effect studies[33b] unambiguously show that the hydrogen transfer can occur via (rate-determining) electron transfer followed by fast proton transfer. (b) Bockman, T. M.; Hubig, S. M.; Kochi, J. K. *J. Am. Chem. Soc.* **1998**, *120*, 2826. (c) As a measure for the solvent polarity, the dielectric constants were taken. See: Murov, S. L.; Carmichael, I.; Hug, G. L. *Handbook of Photochemistry*, 2nd ed.; Dekker: New York, 1993.

(34) Moore, J. W.; Pearson, R. G. *Kinetics and Mechanisms*, 3rd ed.; Wiley: New York, 1981; p 239f.

(35) The equilibrium constant K for diffusional encounters depends on the effective encounter distance *R* between the donor and the acceptor. For the encounter complex between uncharged (spherical) species with $R = 7$ Å, the formation constant is estimated to be $K = 0.9$ M^{-1}. See: Eigen, M. *Z. Phys. Chem. N. F. (Leipzig)* **1954**, *1*, 176.

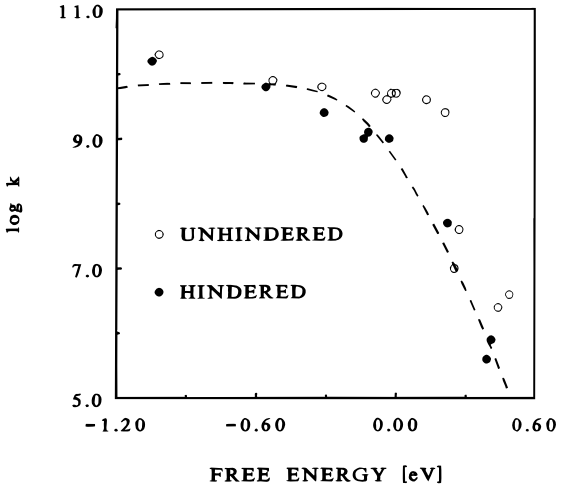

Figure 1. Free-energy dependence of the second-order rate constants of the electron transfer from hindered (●) and unhindered (○) arene donors to photoactivated quinones. The dashed line represents the best fit of the data points of the hindered donors to the Marcus correlation according to eqs 3−5 with $k_{diff} = 8 \times 10^9$ M^{-1} s^{-1}, $Z = 10^{11}$ s^{-1}, $K = 0.86$,[35] $\lambda = 1.2$ eV, and $\alpha = 0.4$ eV.[36e]

B. Unhindered Donors. The kinetics data for the unhindered donor/acceptor pairs (Figure 1, open circles) show significant deviations from the Marcus prediction. Thus, the k_2 values are generally higher than those of the corresponding hindered donor/acceptor pairs, and the points are too strongly scattered in the endergonic ΔG_{ET} region between 0.25 and 0.49 eV for a satisfactory Marcus simulation. To understand these striking effects of steric hindrance, let us now turn to a comparative analysis of the electron-transfer kinetics with hindered and unhindered donors—including studies of the temperature, solvent polarity, and salt effects. We focus on the endergonic and slightly exergonic driving-force region (-0.5 eV $< \Delta G_{ET} <$ 0.5 eV) since it shows the most pronounced effects of steric hindrance, and it is thus particularly informative of the structural requirements in bimolecular electron transfers.

III. Temperature Dependence of the Electron-Transfer Rate Constant. The temperature dependence of the bimolecular ET rate constants for three donor/acceptor pairs that undergo electron transfer with driving forces in the endergonic and slightly exergonic region is presented in Table 4. The two unhindered couples (**CX/DUR)** and (**CA/MES)** show no or very little variation of k_2 over a temperature range of more than 40 °C. Contrastingly, the value of k_2 for the hindered donor/acceptor couple (**CA/TTB)** doubles over a similar temperature range. As such, the Arrhenius plots of ln k_2 versus the reciprocal temperature yield ET activation energies (E_A) of 0, 2.9, and 7.9 kJ mol^{-1} for **CX/DUR**, **CA/MES**, and **CA/TTB**, respectively (see Figure 2). For comparison, Table 4 also contains the activation enthalpies ($\Delta G^{\ddagger}$) for electron transfer as calculated from the ΔG_{ET} values according to Marcus theory.[37] For the two unhindered donor/acceptor pairs, we note a striking discrepancy (up to 30 kJ mol^{-1}) between the experimentally determined activation energies (E_A) and the theoretically predicted $\Delta G^{\ddagger}$ values, whereas E_A for the hindered couple **CA/TTB** is in close agreement with $\Delta G^{\ddagger}$.

Table 4. Temperature Dependence of Electron-Transfer Rate Constants

Q/ArH[a]	CX/DUR	CA/MES	CA/TTB
ΔG_{ET} [eV][b]	+0.21	−0.04	−0.14
k_2 [10^8 M^{-1} s^{-1}][c]			
$T = 239$ K	*d*	*d*	4.4
$T = 253$ K	26.0	32	5.4
$T = 277$ K	26.2	*d*	8.1
$T = 295$ K	25.6	44	9.0
E_A [kJ mol^{-1}][e]	0	2.9	7.9
$\Delta G^{\ddagger}$ [kJ mol^{-1}][f]	30.8	17.4	13.1

[a] Quinone/arene combination (see Charts 1 and 2). [b] Electron-transfer driving force as determined with eq 2. [c] Second-order rate constant for the electron transfer from the arene donor to photoactivated quinone. [d] Not measured. [e] Activation energy as determined from the Arrhenius plot in Figure 2. [f] Free activation enthalpy determined from the Marcus formulation[37] with $\lambda = 77$ kJ mol^{-1}.

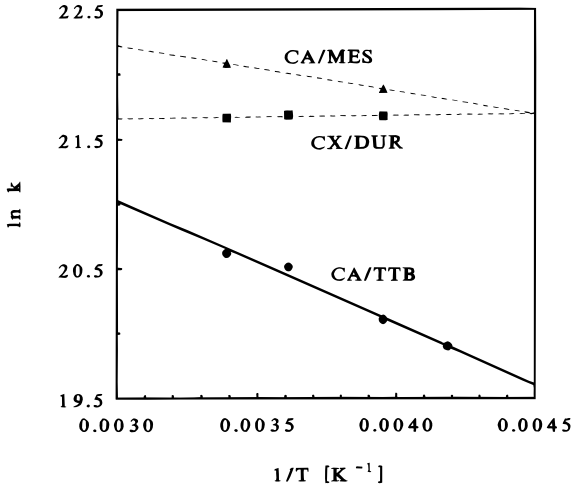

Figure 2. Temperature dependence of the second-order rate constants for electron transfer from **TTB** to **CA*** (●), from **MES** to **CA*** (▲), and from **DUR** to **CX*** (■) evaluated by the Arrhenius relationship. The slopes yield activation energies (E_A) of 7.9, 2.9, and 0 kJ mol^{-1}, respectively.

IV. Comparative Analysis of the Electron-Transfer Kinetics for Hindered and Unhindered Aromatic Donors. A. Curved Versus Linear Kinetics Plots. A striking difference in the kinetic behavior of hindered versus unhindered arene donors is observed when the plots of the observed (first-order) rate constants (k_{obs}) for **Q*** decay are extended to high arene concentrations. Thus the kinetics plots of k_{obs} versus [ArH] for hindered donors remain linear over a wide range of concentrations up to the solubility limits of the arene. By contrast, the kinetics plots for unhindered donors show significant curvature at relatively low donor concentrations, and the k_{obs} values reach limiting (plateau) values at concentrations above 0.2 M. The effect of steric encumbrance on the electron-transfer kinetics is underscored in Figure 3 by the strongly contrasting behavior of durene and its sterically hindered analogue **OMA** in two solvents.

(36) Deviations of the bimolecular ET rate constants from Marcus behavior in the highly exergonic driving-force region ($\Delta G_{ET} < 1.5$ eV) have been observed,[11] and the plateau of diffusion-limited rate constants for highly exergonic electron transfers is taken into account in the empirical free-energy correlation by Rehm and Weller.[11] Various theoretical explanations of the "non-Marcus" behavior (i.e., the lack of the "Marcus-inverted" region) have been reported: (b) Kakitani, T.; Yoshimori, A.; Mataga, N. *J. Phys. Chem.* **1992**, *96*, 5385. (c) Kikuchi, K.; Takahashi, Y.; Katagairi, T.; Niwa, T.; Hoshi, M.; Miyashi, T. *Chem. Phys. Lett.* **1991**, *180*, 403. (d) Gould, I. R.; Young, R. H.; Mueller, L. J.; Farid, S. *J. Am. Chem. Soc.* **1994**, *116*, 8176. (e) To achieve satisfactory overlap between the experimental data and the Marcus simulation, the experimental ΔG_{ET} values of Table 1 were shifted by $\alpha = -0.4$ eV. For a theoretical explanation of the shift parameter α, see: Tamura, S.-I.; Kikuchi, K.; Kokubun, H.; Usui, Y. *Z. Phys. Chem. N. F. (Wiesbaden)* **1978**, *111*, 7.

(37) According to Marcus theory,[13] the activation enthalpy ($\Delta G^{\ddagger}$) is a function of the driving force (ΔG_{ET}) and the reorganization energy (λ) according to: $\Delta G^{\ddagger} = (\lambda/4)(1 + \Delta G_{ET}/\lambda)^2$. The calculation of $\Delta G^{\ddagger}$ in Table 4 is based on $\lambda = 77$ kJ mol^{-1}, as extracted from the Marcus treatment of the data in Figure 1.

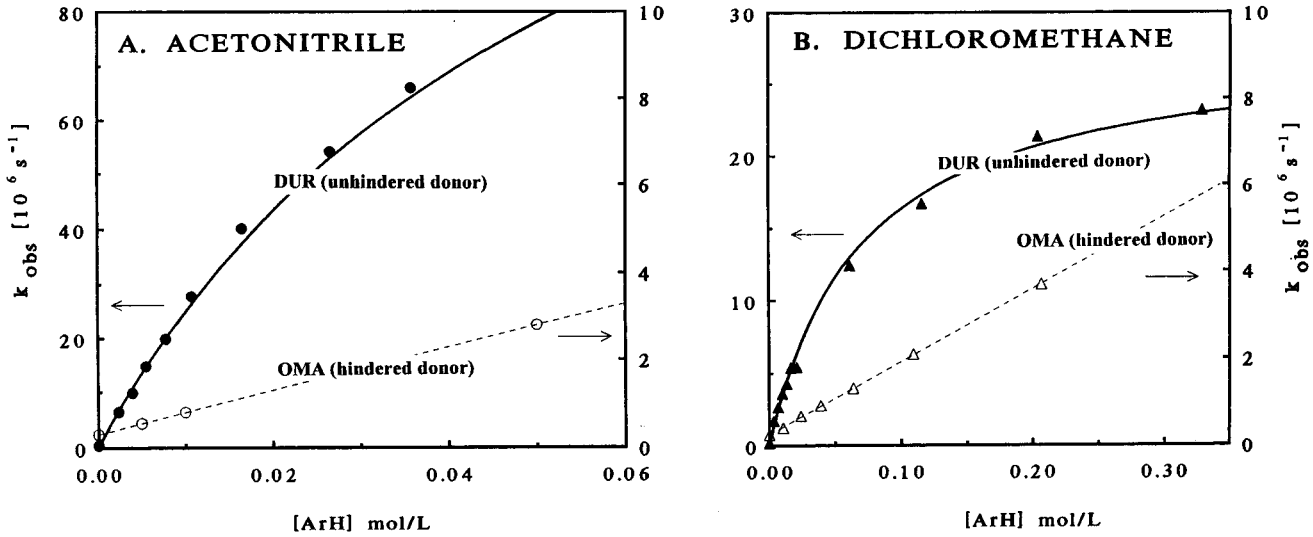

Figure 3. Curved versus linear kinetics plots for electron transfer from durene (filled markers) and its hindered analogue **OMA** (open markers) to photoactivated dichloroxyloquinone in (A) acetonitrile (circles) and (B) dichloromethane (triangles).

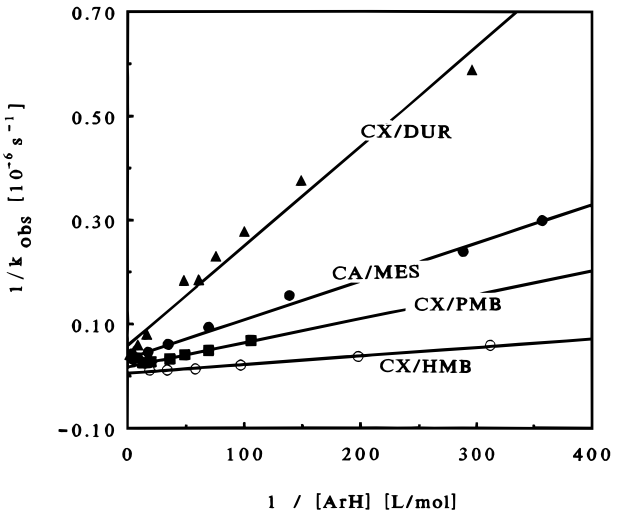

Figure 4. Double-reciprocal representation of the curved kinetics plots in Figure 3 for selected donor/acceptor couples in dichloromethane solution (● = **CA/MES**, ○ = **CX/HMB**, ▲ = **CX/DUR**, and ■ = **CX/PMB**).

The saturation (asymptotic) behavior of k_{obs} (solid circles in Figure 3A and triangles in Figure 3B) is diagnostic of a preequilibrium intermediate[38] between the photoactivated quinone and the aromatic donor prior to electron transfer, and it has been previously identified as the encounter complex,[9] *i.e.*

$$\mathbf{Q^*} + \mathrm{ArH} \underset{}{\overset{K_{EC}}{\rightleftharpoons}} \underset{\text{encounter complex}}{[\mathbf{Q^*}, \mathrm{ArH}]} \xrightarrow{k_{ET}} \mathbf{Q}^{-\bullet} + \mathrm{ArH}^{+\bullet} \qquad (6)$$

Thus, the limiting value of k_{obs} at high donor concentrations corresponds to the intrinsic rate constant (k_{ET}) of the electron transfer within the encounter complex. Accordingly, the curved kinetics plots in Figure 3 are evaluated in a double-reciprocal (linearized) representation in Figure 4, from which the preequilibrium constant (K_{EC}) and the intrinsic electron-transfer rate constant (k_{ET}) are extracted according to eq 7:[39]

$$\frac{1}{k_{obs}} = \frac{1}{k_{ET}} + \frac{1}{K_{EC}k_{ET}}\frac{1}{[\mathrm{ArH}]} \qquad (7)$$

The equilibrium constants (K_{EC}) for complex formation of the various unhindered donors in four solvents are compiled in Table 5. The most striking result of this kinetics evaluation is that the K_{EC} values deviate substantially from the unit value calculated for purely diffusional encounters.[35]

Table 5. Driving-Force Dependence of the Formation Constant (K_{EC}) of the Encounter Complex

			K_{EC} [M^{-1}][c]			
	Q/ArH[a]	ΔG_{ET} [eV][b]	CH_3CN	CH_2Cl_2	$CHCl_3$	CCl_4
1	**CX/MES**	+0.49	1.7	4.0		
3	**CX/XYL**	+0.44	4.3	2.4		
5	**CX/TMB**	+0.27	2.7	4.0		
6	**CA/TOL**	+0.25	2.6	8.7		
7	**CX/DUR**	+0.21	15	14	18	24
9	**CX/PMB**	+0.13	*d*	39		
10	**CX/HMB**	±0	*d*	67	71	202
12	**CA/MES**	−0.04	*d*	30	54	49
14	**CA/XYL**	−0.09	*d*	<10	19	21
16	**CA/DUR**	−0.32	*d*	*d*		
18	**Ca/HMB**	−0.53	*d*	*d*		

[a] Quinone/arene combination (see Charts 1 and 2). [b] Electron-transfer driving force as determined with eq 2. [c] Formation constant (±10%) for the encounter complex [**Q***, ArH]. [d] Not determined due to the linear kinetics plots (see text).

B. Interdependence of k_2, K_{EC}, and k_{ET}. At low arene concentrations, eq 7 simplifies to a linear correlation between k_{obs} and [ArH] to reveal the direct relationship between k_2 (in eq 1) and K_{EC} and k_{ET} (in eq 6), *i.e.*[39c]

$$k_{obs} = K_{EC}k_{ET}[\mathrm{ArH}] = k_2[\mathrm{ArH}] \qquad (8)$$

Thus, the bimolecular rate constants k_2 for electron transfer from ArH to **Q*** can be obtained either from the initial slope of the curved pseudo-first-order plots in Figure 3 or from the slope of the double-reciprocal plots in Figure 4 as the product $K_{EC}k_{ET}$ (see k_2 values in parentheses in Table 1). In other words, the second-order rate constant (k_2) in eq 1 represents a composite

(38) Bunnett, J. F. In *Investigation of Rates and Mechanisms of Reactions*; Part 1; Bernasconi, C. F., Ed.; Wiley: New York, 1986; p 286f.

(39) For a mechanistic description of the limiting kinetics behavior, see: Espenson, J. D. *Chemical Kinetics and Reaction Mechanisms*, 2nd ed.; McGraw-Hill: New York, 1995; p 89f. (b) For the decay kinetics of photoexcited quinones, see: Kobashi, H.; Okada, T.; Mataga, N. *Bull. Chem. Soc. Jpn.* **1986**, *59*, 1975. (c) Note that back electron transfer (k_{-ET}) is neglected in eq 6 on the basis of unit ion yields in Table 1, and the natural decay (k_0) of **Q*** (in the absence of donors) is not included in eq 7 since $k_0 \ll k_{ET}$.[9]

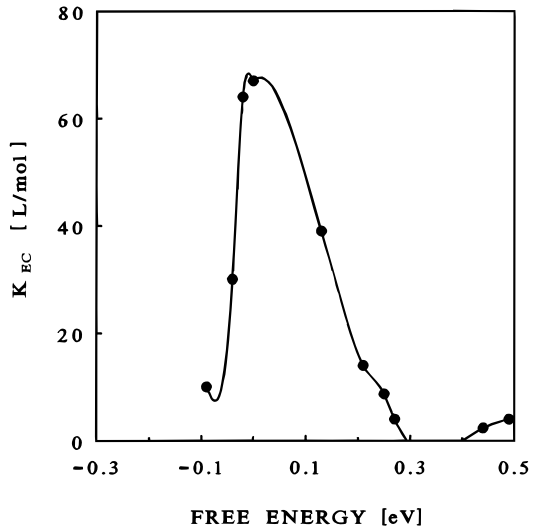

Figure 5. Bell-shaped free-energy dependence of the formation constant K_{EC} of the encounter complex [**Q***, ArH] in dichloromethane.

quantity, each component of which can be affected by the solvent or the driving force.

C. Driving-Force Dependence of K_{EC}. Figure 5 illustrates the unique driving-force dependence of the formation constants listed in Table 5, in which a bell-shaped correlation between K_{EC} and ΔG_{ET} is obtained (in dichloromethane). Particularly noteworthy is that a maximum value of $K_{EC} = 67$ M^{-1} is observed in the isergonic region around $\Delta G_{ET} = 0$ eV, and K_{EC} values close to unity are found in the free-energy regions $\Delta G_{ET} > 0.3$ eV and $\Delta G_{ET} < -0.1$ eV. The data in Table 5 for acetonitrile follow the same trend,[40] and a similar bell-shaped correlation is also observed in chloroform and carbon tetrachloride solution.[9]

Discussion

The comparative study of bimolecular electron transfers from hindered versus unhindered arene donors reveals several striking effects of steric encumbrance which are most pronounced for endergonic and slightly exergonic electron transfers. Electron transfer involving sterically hindered donors meets the conditions of "outer-sphere" electron transfer between weakly coupled donors and acceptors, and can therefore be analyzed according to Marcus theory.[13] On the other hand, electron transfers from unhindered donors do not follow the predictions for "outer-sphere" electron transfer owing to substantial electronic coupling between donor and acceptor, and they are hereinafter referred to as "inner-sphere" processes since the electron transfer occurs via charge-transfer bonds.[41] In other words, the degree of donor/acceptor bonding in the ET transition state is effectively modulated by steric encumbrance as follows.

I. Steric Effects on the Electron-Transfer Kinetics. The kinetics behavior of hindered and unhindered donors is strongly differentiated in Figure 3. The saturation (asymptotic) behavior of the observed rate constants for electron transfer from unhindered donors requires a preequilibrium intermediate prior to electron transfer. This has been previously identified as the encounter complex between arene donor and photoactivated quinone (see eq 6).[9] Thus, the double-reciprocal kinetic evaluation in Figure 4 yields the equilibrium constants for the formation of the encounter complexes which attain values up to $K_{EC} = 200$ M^{-1} (Table 5).[9] Most importantly, the analysis of the spectral features of these donor/acceptor precursors reveals a strong charge-transfer interaction within the transient complex, which has been quantified in terms of its degree of charge transfer $(b/a)^2 \cong 0.3$ or 30%.[6-9]

To achieve such a significant electronic interaction between donor and acceptor orbitals, the (nonbonded) donor/acceptor pair must be arranged in a tight complex to allow optimum coupling of the benzenoid π orbitals. When such a close donor/acceptor association is discouraged by bulky substituents, the charge-transfer interaction within the donor/acceptor pair is precluded.[12] Indeed, chloranil and the unhindered hexamethylbenzene readily form the tight donor/acceptor complex with the van der Waals separation of 3.5 Å (Chart 3), as revealed by X-ray crystallography of charge-transfer crystals.[45] In strong contrast, the closest cofacial approach of chloranil and the hindered hexaethylbenzene of more than 4.5 Å[46] precludes complex formation, and the characteristic charge-transfer absorption is not observed in the sterically hindered donor/acceptor pair.[9,12a,15b]

As a result, only linear kinetics plots are observed for all sterically hindered donor/acceptor combinations, and the formation constants ($K_{EC} \ll 1$) of their encounter complexes are negligibly small. Such small equilibrium constants (K_{EC}) relate to short encounter lifetimes to reduce the overall electron-transfer rates,[47] and result in bimolecular ET rate constants which are at least 10^2 times slower than those of the corresponding unhindered pairs (see Tables 1 and 2).[48] In fact, most rate constants of the hindered donor/acceptor pairs in Tables 1

(40) In acetonitrile, significant curvature in the kinetics plots such as in Figure 3 are only obtained for $\Delta G_{ET} > 0.2$ eV, which allowed us to reliably extract values for K_{EC} and k_{ET} using the reciprocal evaluation in eq 7. The lack of sufficient curvature in the kinetics plots for $\Delta G_{ET} < 0.2$ eV arises from limiting values of k_{obs} which severely exceeded the time resolution of the 10-ns laser pulse ($k_{ET} \gg 10^8$ s^{-1}). See ref 9.

(41) According to our definition (vide supra), inner-sphere mechanisms should be considered in all cases where charge-transfer complexes, exciplexes, or contact ion-radical pairs are actually observed as reaction intermediates.[31,42] In other words, we arbitrarily take electronic interactions in the transition state of less than 1 kcal mol^{-1} (350 cm^{-1}) to result in outer-sphere electron transfer, whereas electronic interactions substantially greater than 350 cm^{-1} lead to inner-sphere electron transfer.[43,44] Accordingly, the outer-sphere/inner-sphere distinction in this study is based on the structure and the critical (spectroscopically established) donor/acceptor orbital overlap in the precursor complex immediately preceding the ET transition state.[9,12a] As a consequence, inner-sphere ET is readily recognized by its unusually fast rates, significant deviations from the Marcus-predicted driving-force dependence, and pronounced sensitivity to steric hindrance. For earlier studies, see: (a) Fukuzumi, S.; Wong, C. L.; Kochi, J. K. *J. Am. Chem. Soc.* **1980**, *102*, 2928. (b) Fukuzumi, S.; Kochi, J. K. *Bull. Chem. Soc. Jpn.* **1983**, *56*, 969. (c) Kochi, J. K. *Angew. Chem., Int. Ed. Engl.* **1988**, *27*, 1227.

(42) For inner-sphere descriptions of ion-pair states, see: (a) Hubig, S. M.; Bockman, T. M.; Kochi, J. K. *J. Am. Chem. Soc.* **1996**, *118*, 3842. (b) Bockman, T. M.; Karpinski, Z. J.; Sankararaman, S.; Kochi, J. K. *J. Am. Chem. Soc.* **1992**, *114*, 1970. (c) Hörmann, A.; Jarzeba, W.; Barbara, P. F. *J. Phys. Chem.* **1995**, *99*, 2006.

(43) Reynolds, W. L.; Lumry, R. W. *Mechanisms of Electron Transfer;* Ronald Press: New York, 1966; p 12.

(44) Typical examples for inner-sphere mechanisms involving organic substrates are as follows: (a) Oxidation of alkylbenzenes by nitrate radical ($NO_3^{\bullet}$): Del Giacco, T.; Baciocchi, E.; Steenken, S. *J. Phys. Chem.* **1993**, *97*, 5451. (b) Reduction of nitroarenes by oxygen atom transfer to Ru−carbonyl complexes: Skoog, S. J.; Gladfelter, W. L. *J. Am. Chem. Soc.* **1997**, *119*, 11049. (c) Reduction of methyl iodide by HI: Holm, T.; Crossland, I. *Acta Chem. Scand.* **1996**, *50*, 90.

(45) Harding, T. T.; Wallwork, S. C. *Acta Crystallogr.* **1955**, *8*, 757.

(46) Based on molecular-mechanics calculations in ref 12a.

(47) For example, a unit equilibrium constant ($K = k_{diff}/k_{-diff} = 1$ M^{-1}) and a diffusion-controlled rate constant ($k_{diff} = 2 \times 10^{10}$ M^{-1} s^{-1}) for the formation of the encounter complex result in a dissociation constant of $k_{-diff} = 2 \times 10^{10}$ s^{-1}, which corresponds to a lifetime of 50 ps. See also: Marcus, R. A. in ref 6a.

(48) For steric effects on other photoinduced electron transfers, see: (a) Jones, G., II; Chatterjee, S. *J. Phys. Chem.* **1988**, *92*, 6862. (b) Gassman, P. G.; DeSilva, S. A. *J. Am. Chem. Soc.* **1991**, *113*, 9870. (c) Gould, I. R.; Farid, S. *J. Phys. Chem.* **1993**, *97*, 13067.

Chart 3

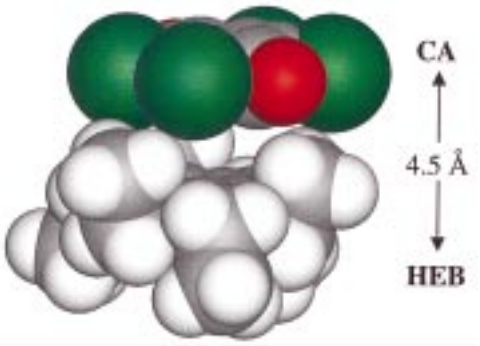

and 2 are several orders of magnitude slower than those for diffusion-limited processes ($k_{diff} \cong 10^{10}$ M^{-1} s^{-1}),[34] which indicates that only a small fraction of the quinone/arene (collisional) encounters endure long enough to undergo electron transfer.

II. Steric Effects on the Temperature and Solvent Dependence of the Bimolecular Rate Constants. To further amplify the difference between the ET mechanisms of hindered and unhindered donors, let us now consider temperature and solvent effects.

A. Temperature Effect. The absence of a significant temperature dependence on the ET rate constants of unhindered donors in Figure 2 and Table 4 indicates ET activation energies (E_A) close to zero. This finding is in striking contrast to the "outer-sphere" electron-transfer model that predicts a quadratic variation of the activation enthalpy ($\Delta G^{\ddagger}$) with the free-energy change (ΔG_{ET}) for electron transfer.[13] Thus, on the basis of reasonable reorganization energies extracted from the Marcus simulation in Figure 1,[37] we calculate activation enthalpies ($\Delta G^{\ddagger}$) that are up to 30 kJ mol^{-1} higher than the experimental data for E_A in Table 4. The lack of temperature effects and the low activation energies follow from the preequilibrium formulation in eq 6. In other words, unusual temperature effects on the overall reaction kinetics are expected when complex formation precedes electron transfer.[49] As a result, even strongly endergonic electron transfers (as described in this study) may exhibit negligible activation energies due to an opposing temperature dependence of complex formation (and the follow-up electron transfer). For example, we previously demonstrated that the temperature independence of k_2 for the **CX**/**DUR** couple in Table 4 results from an increase of K_{EC} and compensating decrease of k_{ET}.[9] On the other hand, electron transfers with sterically encumbered donors show normal temperature effects and reasonable activation energies (see Table 4)—supporting the foregoing conclusion that donor/acceptor complexes are unimportant. *In other words, bimolecular electron transfers of sterically encumbered donors follow the predicted behavior of "outer-sphere" electron transfer between weakly coupled donors and acceptors.*[13]

B. Solvent Effect. Solvent variation on the ET rate constants of hindered versus unhindered donors provides further distinction of the reaction mechanisms. Thus the moderate solvent effect on unhindered donor/acceptor pairs in Table 2 is similar to that previously observed for back-electron transfer in contact ion pairs[50] or for intramolecular electron-transfer processes.[51] In both cases, quantum-mechanical tunneling due to high-frequency modes can account for the lack of solvent effects.[50] By contrast, the striking difference in Figure 3 on hindered donor/acceptor couples establishes the important role of the solvent in differentiating electron-transfer pathways. Such a critical involvement of the solvent molecules can only be envisioned for "loose" encounters between donors and acceptors that characterize the "outer-sphere" electron-transfer model.

C. Salt Effects. The significant effects of added salt on the ET rates of hindered donor/acceptor couples in chloroform (in Table 3) are similarly interpreted as electron transfers within "loose" encounters of the donors being susceptible to ionic strength for ion-radical stabilization in solution.[52]

III. Steric Effects on the Free-Energy Correlation of the Electron-Transfer Rate and Role of the Encounter Complex. The difference in the ET mechanisms between hindered and unhindered donor/acceptor pairs is most evident in the comparison of the free-energy correlations in Figure 1. Thus, the rate constants for the hindered donor/acceptor pairs are readily accommodated by Marcus theory, particularly in the endergonic and slightly exergonic free-energy region.[36] Contrastingly, the rate constants for unhindered donor/acceptor combinations are scattered in the same free-energy range and are not well fitted to reasonable Marcus parameters. Similar deviations from Marcus behavior were previously observed for endergonic and slightly exergonic electron transfers from photoactivated pyrene (or naphthalene) to cyanoarene acceptors.[49a] Furthermore, the absence of significant temperature dependence of the ET rate constants was evidence for strong (donor/acceptor) complexation prior to electron transfer. [49a, 53]

The ET rate constants of unhindered donor/acceptor couples are *faster* than those of the hindered analogues. They are also *faster* than those predicted by Marcus theory, and the greatest deviation from Marcus behavior is observed for donor/acceptor couples that form the strongest encounter complexes. This discrepancy is illustrated in Figure 6 by the superposition of the ET rate constants of the unhindered donors from Figure 1 with the formation constants for encounter complexes from Figure 5 as a function of the driving force. It is particularly noteworthy that the fast ET rate constants observed for unhindered donors coincide with the maximum in the formation constant. As a result, such tight encounter complexes with strong charge-transfer character must experience a significant predisposition toward electron transfer,[9] which allows even endergonic

(49) Baggott, J. E.; Pilling, M. J. *J. Chem. Soc., Faraday Trans. 1* **1983**, *79*, 221. (b) See also: Baggott, J. E. In *Photoinduced Electron Transfer*; Fox, M. A., Chanon, M., Eds.; Elsevier: New York, 1988; Part B, p 385f.

(50) Asahi, T.; Ohkohchi, M.; Mataga, N. *J. Phys. Chem.* **1993**, *97*, 13132.

(51) Asahi, T.; Ohkohchi, M.; Matsusaka, T.; Mataga, N.; Zhang, R. P.; Osuka, A.; Maruyama, K. *J. Am. Chem. Soc.* **1993**, *115*, 5665.

(52) Gordon, J. E. *The Organic Chemistry of Electrolyte Solutions;* Wiley: New York, 1975; p 99f. (b) Masnovi, J. M.; Kochi, J. K. *J. Am. Chem. Soc.* **1985**, *107*, 7880. (c) Yabe, T.; Kochi, J. K. *J. Am. Chem. Soc.* **1992**, *114*, 4491.

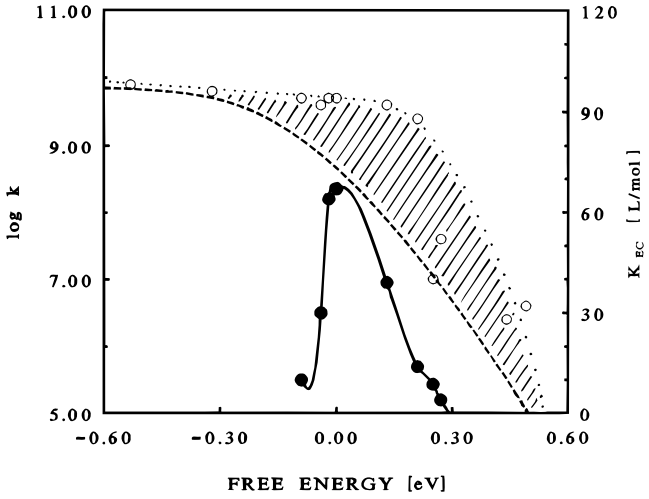

Figure 6. Superposition of Figures 1 and 5 to demonstrate the coincidence of the maximum for encounter-complex formation (●) and the maximum deviation of the data with unhindered donors (○) from the Marcus simulation (dashed line).

electron transfers to occur at diffusion-limited rates (see Figure 1 and Table 1).[54] In contrast, sterically encumbered donors are subject to rather "loose" diffusive encounters with the photoactivated quinones at intermolecular distances greater than 4.5 Å—sufficient to discourage any significant charge-transfer interaction prior to electron transfer.[12a] Thus, these electron-transfer couples represent optimum donors for purely "outer-sphere" electron transfer.[55] On the other hand, the electron donors with little or no steric encumbrance cannot meet the criterion for "outer-sphere" electron transfer since they form encounter complexes with a considerable degree of charge-transfer or inner-sphere bonding. As such, we envisage steric encumbrances as an important modulating influence on the changeover from outer-sphere to inner-sphere pathways in electron-transfer mechanisms of aromatic donors.[56] Both types of electron transfers ultimately result in the same electron-transfer *products* (viz. ion-radical pairs) without any overall changes in intermolecular chemical bonding.[57] Thus, we expect the mechanistic difference in the degree of bonding in the precursor complexes immediately preceding the transition states to greatly affect the electron-transfer rate constant and its dependence on the driving force, the temperature, and the solvent.

Summary and Conclusions

Steric effects on the kinetics of electron transfer from hindered and unhindered arene donors to quinone acceptors and their temperature, solvent, and driving-force dependence reveal a structure-induced (mechanistic) changeover. Thus unhindered donors undergo inner-sphere electron transfer[28−30] owing to the strong electronic coupling of donor and acceptor in a well-defined encounter complex preceding the ET transition state. By contrast, hindered donors show no (kinetic or spectroscopic) evidence for a discrete encounter complex in the preequilibrium step, and the kinetics follows outer-sphere ET behavior expected for weakly coupled donors and acceptors.[13] Although this comparative study of hindered and unhindered electron donors establishes a clear-cut (experimental) distinction between outer-sphere and inner-sphere electron transfers, we believe there will generally be a broad borderline region between the two mechanisms.[30e] Thus the idealized descriptions of inner-sphere and outer-sphere should be taken as the two extreme ends of a continuum of electron-transfer behavior that is tuned by the magnitude of electronic coupling of the donor/acceptor pairs.[30]

Experimental Section

Materials. Hexaethylbenzene (Acros), hexamethylbenzene, pentamethylbenzene, durene, 1,3,5-tri-*tert*-butylbenzene, 3,5-di-*tert*-butyltoluene, and 1,4-di-*tert*-butylbenzene (Aldrich) were recrystallized from ethanol and heptane. Mesitylene, *p*-xylene, and 1,2,4-trimethylbenzene (Aldrich) were purified by distillation. Tetrachloro-*p*-benzoquinone (chloranil, Aldrich) was sublimed in vacuo and recrystallized from benzene. Toluene (reagent grade) was distilled from sodium and benzophenone under an argon atmosphere. 1,1,4,4,5,5,8,8-Octamethyl-1,2,3,4,5,6,7,8-octahydroanthracene was synthesized according to the literature procedure.[58] The synthesis of 2,5-dichloroxyloquinone,[9] as well as that of pentaethyltoluene and triethylmesitylene,[12a] was reported earlier. Dichloromethane, acetonitrile, chloroform, and carbon tetrachloride were purified according to standard procedures.[59] The laser photolysis experiments were carried out with the third harmonic (355 nm) output of a Q-switched Nd:YAG laser (10-ns fwhm, 22 mJ) for the generation of the triplet quinones, and the details have been described earlier.[60]

Determination of Ion-Radical Yields. The ion-radical yields in Table 1 were obtained with benzophenone as the transient actinometer.[61] Samples of quinone/donor combinations in acetonitrile and benzophenone in benzene with matching absorbance at 355 nm were exposed to the 10-ns laser pulses, and the transient absorbance of triplet

(53) However, the electron-transfer rate constants of the pyrene/cyanoarene systems were found to be *slower* than those predicted by Marcus theory for "outer-sphere" electron transfer. As such, reaction pathways other than electron transfer were invoked to account for the low rate constants of fluorescence quenching of pyrene and naphthalene by cyanoarenes. In our study, the ion-radical yields of unity for most donor/acceptor couples (see Table 1) rule out such alternative pathways.

(54) A more physical view accounts for the fast rate constants in inner-sphere electron transfer by its adiabatic pathway. Thus, strong electronic coupling between the donor and the acceptor in close (van der Waals) distance leads to an avoided crossing of the potential surfaces. A substantial energy gap of $\Delta\epsilon = 2H_{AB}$ results in adiabatic electron transfer with unit probability. See: Marcus, R. A.; Sutin, N. *Biochim. Biophys. Acta* **1985**, *811*, 265.

(55) In these electron transfers, the weak electronic coupling between the sterically encumbered redox partners leads (in its extreme) to a nonadiabatic (diabatic) electron transfer that (in the isergonic and endergonic driving-force region) results in very slow rates. For examples of nonadiabatic electron transfers due to steric hindrance, see: (a) Rau, H.; Frank, R.; Greiner, G. *J. Phys. Chem.* **1986**, *90*, 2476. (b) Sandrini, D.; Maestri, M.; Belser, P.; Von Zelewski, A.; Balzani, V. *J. Phys. Chem.* **1985**, *89*, 3675. (c) Koval, C. A.; Pravata, R. L. A.; Reidsema, C. M. *Inorg. Chem.* **1984**, *23*, 545. (d) Koval, C. A.; Ketterer, M. E. *J. Electroanal. Chem.* **1984**, *175*, 263. (e) Kitamura, N.; Rajagopal, S.; Tazuke, S. *J. Phys. Chem.* **1987**, *91*, 3767.

(56) In the strongly exergonic driving-force region, the electron-transfer behavior of hindered versus unhindered donors cannot be distinguished experimentally (i.e., all rate constants are at the diffusion limit), which may indicate the merging of inner-sphere and outer-sphere mechanisms. Under these energetic conditions, electron transfer is apparently faster than diffusion even at donor/acceptor distances of 4.5 Å and more. This observation suggests that, with increasing driving force of the electron transfer, the effective electron-transfer distance also increases, and electron transfer remains competitive with diffusion. [The lack of "Marcus-inverted" behavior in bimolecular electron transfers has been explained on the basis of this effect.[36b]] Accordingly, the observation of steric effects on the rate constants for bimolecular electron transfers in the highly exergonic driving-force region (and possibly the observation of the Marcus-inverted region) is only expected at driving forces and donor/acceptor distances at which the electron transfer is the rate-limiting step following the diffusional formation of the encounter complex. Other explanations for the lack of an inverted driving-force dependence of bimolecular electron-transfer rate constants in the exergonic region are cited in ref 36. The possibility of observing the inverted region in extremely hindered organic donors/acceptors is under investigation.

(57) The electron transfer does not effect any net bond formation or bond cleavage in either reactant. Moreover, back electron transfer in acetonitrile solution completely restores the starting donor/acceptor pairs.

(58) Bruson, H. A.; Kroeger, J. W. *J. Am. Chem. Soc.* **1940**, *62*, 36.

(59) Perrin, D. D.; Armarego, W. L. F. *Purification of Laboratory Chemicals*, 3rd ed.; Pergamon: Oxford, 1988.

(60) Bockman, T. M.; Karpinski, Z. J.; Sankararaman, S.; Kochi, J. K. *J. Am. Chem. Soc.* **1992**, *114*, 1970.

benzophenone at 525 nm ($\epsilon_{525} = 7{,}220\ M^{-1}\ cm^{-1}$)[61] was quantitatively compared with that of the chloranil anion radical at 450 nm ($\epsilon_{450} = 9700\ M^{-1}\ cm^{-1}$)[62] or that of the **CX** anion radical at 430 nm ($\epsilon_{430} = 6800\ M^{-1}\ cm^{-1}$).[9] For comparison, the absorption bands of the arene cation radicals were also examined to ensure sufficient separation from the quinone anion-radical absorption.

Kinetics Measurements. A 0.005 M solution of quinone in acetonitrile (or dichloromethane, chloroform, or carbon tetrachloride) was exposed to 355-nm (10-ns) laser excitation, and the decay of the triplet quinone was observed at 500 nm on the ns/μs time scale in the presence of varying concentrations (10^{-4} to 10^{-1} M) of aromatic donors. The transient decay was fitted to first-order kinetics, and the observed rate constants (k_{obs}) were plotted against the donor concentration. The slope of the linear portion of the pseudo-first-order plots in Figure 3 yielded the second-order rate constants (k_2, ±10%) in Tables 1−4 according to eq 8. The kinetics of the curved plots of the unhindered donors was evaluated with eq 7 by considering the preequilibrium step in eq 6 to obtain the equilibrium constants K_{EC} in Table 5 and Figure 5. For additional details of the kinetics analysis, see Rathore et al. in ref 9 and references therein.

Acknowledgment. We thank the National Science Foundation and the R. A. Welch Foundation for financial support.

JA9831002

(61) Hurley, J. K.; Sinai, N.; Linschitz, H. *Photochem. Photobiol.* **1983**, *38*, 9.

(62) André, J. J.; Weill, G. *Mol. Phys.* **1968**, *15*, 97.